Journal of Magnetism and Magnetic Materials 623 (2025) 172965

Contents lists available at ScienceDirect

Journal of Magnetism and Magnetic Materials

journal homepage: www.elsevier.com/locate/jmmm

Research article

Experimental estimation of the remanent induction for the study of functional fatigue in permanent magnets

Abderraouf Ouazib[1], Mathieu Domenjoud[*,1], Laurent Daniel[1]

Université Paris-Saclay, CentraleSupélec, CNRS, Laboratoire de Génie Electrique et Electronique de Paris, Gif-sur-Yvette, 91192, France
Sorbonne Université, CNRS, Laboratoire de Génie Electrique et Electronique de Paris, Paris, 75252, France

ARTICLE INFO

Keywords:
Functional fatigue
Cyclic mechanical stress
Permanent magnet
Remanent magnetization
Extraction method

ABSTRACT

The magnetization of new generation hard ferromagnetic materials is difficult to access experimentally without the use of advanced and expensive instruments. This article proposes two novel, easily implementable techniques for measuring the remanent induction of permanent magnets: a variant of the extraction method and a residual magnetic field method. Both methods are validated on hard Ferrites by comparison with hysteresis loop measurements taken as a reference measurement. The advantages and disadvantages of each method are discussed. Subsequently, the proposed techniques are applied to measure the remanent induction of rare-earth magnets, specifically Neodymium–Iron–Boron (Nd–Fe–B) and Samarium-Cobalt (Sm-Co). The obtained results exhibit consistency with manufacturer-provided data, attesting to the accuracy of the proposed measurement methodologies. Furthermore, the research investigates the effect of cyclic mechanical loading on the remanent induction of permanent magnets. The magnets are subjected to a set of 10^6 sinusoidal uniaxial compression cycles at a frequency of 30 Hz and at stress amplitudes representative for practical conditions in electrical machine applications. The remanent induction of the mechanically cycled magnets is subsequently measured. The investigation reveals no significant fatigue effect on the remanent induction in the studied hard materials. Overall, this study provides insights into the magneto-mechanical coupling effects in hard ferromagnetic materials and into the performance analysis of magnet properties under time-varying mechanical loadings.

1. Introduction

Magnets exhibit a unique ability to generate a permanent magnetic field, enabling the development of various electromagnetic devices. Permanent magnets are found, for instance, in electrical motors and generators, sensors and detectors, speakers and headphones [1]. The remanent induction of permanent magnets directly affects the performance of motors, so that a precise measurement of remanent induction is key to the design and optimization of electrical machines [2,3].

In many applications, magnets are put in harsh thermal and mechanical conditions. In high speed permanent magnet synchronous machines (PMSM), for instance, the distribution of mechanical stresses in the rotor must be considered to ensure mechanical reliability [4–6]. In order to provide the required performance without exceeding the yield stress of the constituent materials, the stress distribution must be evaluated in every part of the rotor, including the permanent magnets.

Due to their low resistance to tensile stress, permanent magnets are usually pre-compressed in the rotor. This compression can be obtained in different ways. A glass- or carbon-fiber retention sleeve can be used in surface-mounted PMSM [4]. In the case of buried magnets rotors, either the rotor iron itself fixes the magnets [4], or an enclosure is specifically designed for this purpose [5]. Borisavljevic et al. [5] evaluated stress on a Neodymium–Iron–Boron (Nd–Fe–B) magnet in a high-speed disc-shaped motor application (targeted speed of 200 000 rpm) and found it to vary from −127 MPa at rest to −13.1 MPa at full speed (compressive stress states). These severe mechanical loadings raise questions about their effects on the properties of the magnetic materials. The study of these effects requires advanced magnetic characterization of hard ferromagnets.

This article focuses on the effect of cyclic stress on the properties of permanent magnets for electrical engineering applications. Methods for measuring the remanent induction of hard ferromagnetic materials are presented first, and two novel methods are introduced. In the second part, the evolution of the permanent magnet properties under cycling

* Correspondence to: Laboratoire de Génie Électrique et Électronique de Paris, Université Paris-Saclay - CentraleSupélec - CNRS - Sorbonne Université, 11 rue Joliot-Curie - GeePs, 91192 Gif sur Yvette, France.
E-mail addresses: abderraouf.ouazib@centralesupelec.fr (A. Ouazib), mathieu.domenjoud@centralesupelec.fr (M. Domenjoud), laurent.daniel@centralesupelec.fr (L. Daniel).

[1] All authors have read and agreed to the published version of the manuscript.

https://doi.org/10.1016/j.jmmm.2025.172965
Received 6 September 2024; Received in revised form 3 March 2025; Accepted 12 March 2025
Available online 25 March 2025

mechanical loading, also known as functional fatigue, is studied on three classes of permanent magnets.

2. Measuring the remanent induction of magnets

The main characterization methods for hard magnetic materials and the various issues that arise when applying these methods are reviewed in [7,8]. The closed-circuit fluxmetric method is one of the most commonly used techniques for characterizing the behavior of ferromagnetic materials. The normative frame for using this method for hard ferromagnetic materials is described in [9]. However, the coercive fields of permanent magnets can be very high (around 1.5×10^6 A/m, or even higher for rare-earth-based magnets), and the saturation fields are close to 5×10^6 A/m. Such values are very challenging for applying the fluxmetric method [10].

Various open-circuit methods for characterizing magnetic materials have been proposed in the literature [10–12]. This study focuses on methods that allow the estimation of the remanent induction B_r without applied magnetic field. The extraction method [13] is the most common. It consists in passing the magnet through the cross-section of a coil and measuring the induced voltage. It is mainly applicable to cylindrical or parallelepiped-shaped samples but becomes challenging for samples with small length due to the difficulty of obtaining an adequate winding. Other authors were inclined to identify a relation between the samples magnetization and the corresponding surrounding magnetic field, measured with a Hall probe and from a far distance so that the sample can be assimilated to a magnetic dipole [14].

In this work, two methods for evaluating the remanent induction of magnets are proposed. The first one is a modified extraction method (MEM), which is applicable to samples with small lengths and suitable for closed-circuit magnetic characterization setups. The second one is a residual magnetic field method (RMFM) using a Hall probe. The conventional extraction method is first presented to provide a basis for describing the proposed variant (MEM), which is described next. The method for determining the demagnetization coefficient, necessary for applying this method, is also described. A comparison between the results obtained with the MEM and with the fluxmetric method serves as a validation in the case of a hard Ferrite. The second method (RMFM) is then presented and validated by comparison to both the fluxmetric method and numerical modeling results. Finally, the two proposed methods, MEM and RMFM, are applied to Neodymium–Iron–Boron (Nd–Fe–B) and Samarium-Cobalt (Sm–Co) permanent magnets for which the fluxmetric method is not easily implementable.

2.1. Classical extraction method

The extraction method is a standard method for the measurement of the remanent induction of permanent magnets [13]: the magnet is moved from a resting position, where it is fully inserted into a short detection coil, to a distant location where the flux created by the magnet and passing through the coil is zero [10]. If the cross-section of the measuring coil is adjusted to be identical to the cross-section of the sample S, the initial magnetic flux is equal to $\Phi_i = \mu_0 (M_r + H_d^f) S$, where M_r is the remanent magnetization to be measured (assumed uniform within the magnet), μ_0 is the vacuum magnetic permeability, and H_d^f is the average demagnetizing field in the midplane perpendicular to the magnet axis.

The demagnetizing field H_d is related to the magnetization of the sample by the demagnetization coefficient N_d. Strictly-speaking, this coefficient is rigorously defined only in the case where magnetization M and demagnetizing field H_d are uniform. Except for uniformly magnetized ellipsoids, it is not generally the case. An average demagnetizing coefficient across the mid-section of the magnet (fluxmetric demagnetizing coefficient N_d^f) is defined for the case of a short detection coil. It relates the average demagnetizing field in the mid-section to the supposedly uniform magnetization M_r via the relation $H_d^f = -N_d^f M_r$. Considering that the final flux (when the sample is sufficiently far from the measuring coil) is zero, the variation of flux through the coil can be written as:

$$\Delta\Phi = -\mu_0 M_r \left(1 - N_d^f\right) S. \tag{1}$$

The solution proposed in the literature for the case of short samples [10,11], is to use the principle of reciprocity, which relates the magnetization of the sample to the flux variation in a detection coil placed close to the small sample. The flux variation is generated by moving the sample from the test zone (defined by the geometrical properties of the coil with a field uniformity of at least 1%) to a zone where the flux through the coil is zero. This solution requires a precise sizing of the detection coil, permitting an accurate determination of the coil constant k_B defined by the ratio between the magnetic induction B measured at the test zone and the current I in the coil ($k_B = B/I$), so that an accurate determination of the test zone is possible [10,11,13]. The obtained relation for a uniformly magnetized sample is then:

$$\Delta\Phi = k_B V M_r \tag{2}$$

where V is the sample volume.

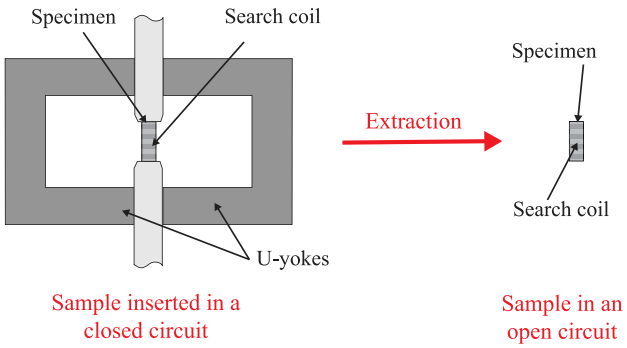

Fig. 1. Modified extraction method (MEM) setup.

2.2. Modified extraction method (MEM)

The proposed variation of this method, illustrated in Fig. 1, involves measuring the flux variations through a coil wounded around the permanent magnet covering its entire lateral surface (note that if the entire lateral surface is not covered by the coil, the approach is still applicable, adjusting the calculation of the demagnetization factor to the region covered by the coil).

The flux variation is measured during the extraction of the coil and magnet assembly from a closed circuit. This closed circuit consists of two columns of Permendur 49, with a flux closure by two yokes of soft Ferrite. For the experiments conducted in this work, the effective cross-sectional area is 400 mm^2 for the columns, and 560 mm^2 for the yokes. The effective magnetic path length of each side of the formed magnetic circuit is 252 mm. Such a configuration eliminates the relative movement between the sample and the coil, and permits to bypass the problems related to the sizing of the detection coils and the determination of the test zone encountered with the usual extraction method.

Assuming a complete absence of demagnetizing effects in the closed circuit, the initial flux is $\Phi_i = \mu_0 M_r S$. The final flux is $\Phi_f = \mu_0 M_r (1 - N_d^m) S$, after the sample is removed from the circuit and the magnetic induction is reduced due to the demagnetizing field. Again here, there is no rigorous definition of the demagnetizing factor, and the magnetometric demagnetizing coefficient N_d^m is used. It is defined as the average demagnetizing coefficient over the entire volume of the sample, assumed to be uniformly magnetized. The measured flux

variation $\Delta\Phi$ corresponds to the difference between these two flux values. The remanent magnetization M_r can be deduced from the measurement of $\Delta\Phi$:

$$M_r = -\frac{\Delta\Phi}{\mu_0\ N_d^m\ S}. \tag{3}$$

Practically, the measurement of $\Delta\Phi$ is done by numerically integrating the induced voltage recorded at the ends of the coil wound around the sample. The demagnetizing factor N_d^m can be obtained numerically (see Appendix A).

2.3. Validation of the MEM

The validation of the MEM is performed by comparison to the fluxmetric method. A hard Ferrite is selected for this purpose. This material possesses a sufficiently high coercive field to resist its own demagnetizing field, but low enough to perform a hysteresis loop in a closed circuit. The measurements were done on a 10 mm-diameter and 10 mm-height cylindrical sample.

The experimental setup used is the closed circuit described in Fig. 1, where excitation coils are added around the sample. The magnetization of the material is achieved by an applied current in a series circuit of four primary coils (16 AWG wire) attached to a power amplifier, one wound around each yoke (600 turns each) and two around the columns (265 turns each). The magnetic induction is measured via a detection coil wound around the sample (50 turns). A dSPACE module stores and processes experimental data, at a sampling frequency of 50 kHz. The magnetic field is measured with a Hall probe (a transverse probe BTP 201-F75 with the "BROCKHAUS Gaussmeter BGM 201" used in the measuring range of 400 mT) placed in immediate proximity to the sample. More details about the experimental setup and estimation of measurement errors can be found in [15]. This circuit forms the closed loop configuration that allows for magnetizing the material, for the induction measurement, and in turn, for acquiring the hysteresis loops.

The remanent induction of the magnet sample is obtained using three methods:

- using the MEM,
- using a full hysteresis loop (and recording the intersection with the B-axis at $H = 0$),
- using an initial magnetization curve.

In the absence of H_d, $B_r = \mu_0\ M_r$.

Additional details on the measurement from an hysteresis loop are provided in Appendix B. This technique shows very small uncertainty, in connection with three main sources:

- the error on the estimation of the sample section, responsible of errors up to 0.1 mT on the induction B,
- the small drift on the signal due to the integration process for the determination of B. This drift was estimated empirically to create errors of the order of 0.5 mT on the induction B,
- a repeatability error representing 0.2% of the measured value for the induction B.

The measurement from the initial magnetization curve involves using a demagnetized sample (see [15,16] for a detailed description of the demagnetization procedure). It consists in measuring the magnetic induction from the demagnetized state until a maximum value and the subsequent return to the remanent state. The final value of the induction corresponds to the remanent induction B_r. The error levels for this technique are larger than for the hysteresis loop method. They have the same three origins but the estimated repeatability is larger in this case, because of the sensitivity of the technique to the initial magnetization level of the sample, leading to an error estimated empirically around 1% due to the imperfect demagnetization of the sample.

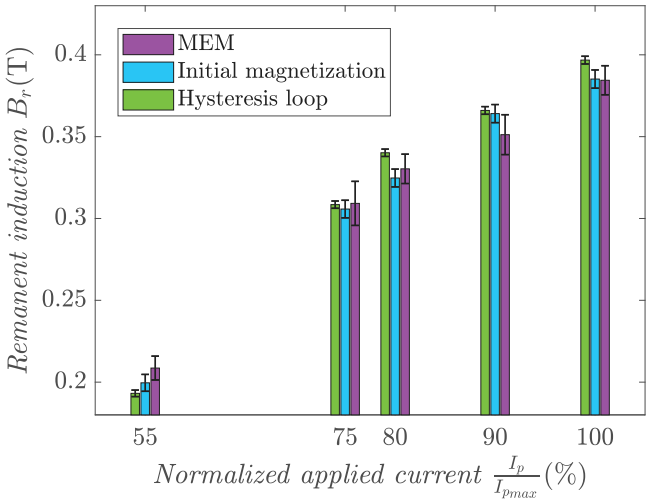

Fig. 2. Comparison of the measurement of remanent induction B_r obtained with the modified extraction method (MEM), and using two classical magnetic measurements in a closed circuit for a hard Ferrite and for various values of normalized current (55%, 75%, 80%, 90%, 100%). I_p represents the applied peak current and I_{pmax} the applied peak current required to obtain a major loop.

The MEM presents also the same three sources of errors. Nevertheless, the section estimation and drift are negligible compared to the repeatability error. Each measurement was repeated at least five times for this method, so that the repeatability error is represented in the error bar. Numerical simulation of the circuit has shown that the relative error in estimating B_r without accounting for the demagnetizing field H_d in the closed-circuit configuration is less than 0.25%.

The three techniques were applied to a sample after reaching five levels of maximum induction from the demagnetizing state (from 55% to 100% of the maximum induction). Fig. 2 shows the corresponding results for B_r. The results obtained from the MEM measurements are well repeatable, with a relative standard deviation not exceeding 4%. The results obtained from the hysteresis loop method exhibit the smallest repeatability error. Comparing the MEM results to the hysteresis loop measurement, the MEM results show relative deviations of less than 4% for inductions close to the maximum value of B_r. An overestimation of the result (8%) is observed at low induction. This can be attributed to the heterogeneity of the magnetization in the sample, limiting the validity of the expression for the demagnetizing factor N_d. The measurement from the initial magnetization requires a demagnetization of the sample. The quality of the demagnetization may vary from one measurement to another, and consequently represents an additional error source (note that the applied demagnetizing procedure ensures a demagnetization at an induction level not exceeding 2% of the saturation induction of the sample). As shown in Fig. 2, all the initial magnetization measurements fall into the error bars of the MEM measurements, which is another validation of the MEM. From these measurements, errors not exceeding 4% are expected from MEM when magnetization is uniform and the sample is initially placed in a closed circuit with no air gaps.

2.4. Residual magnetic field method (RMFM)

A second method for measuring the remanent induction of cylindrical magnets is proposed. It consists in measuring, using a Hall probe, the magnetic field in immediate proximity to the top and bottom surfaces of the magnet, generated by the presence of the remanent magnetization in the sample. This magnetic field is noted residual magnetic field H_{res}. The active zone of the probe (around 1 mm^3) is placed in the central zone of the surface where the measured field is uniform. The Hall probe used in this study is a BTP 201-F75 transverse

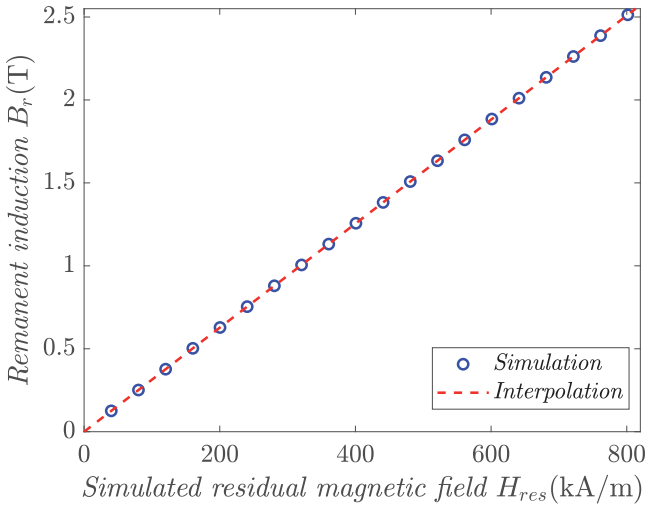

Fig. 3. Simulated residual field versus remanent induction for a 10 mm-diameter 10 mm-height cylinder with recoil permeability $\mu_{rec} = 1$ at different levels of remanent inductions.

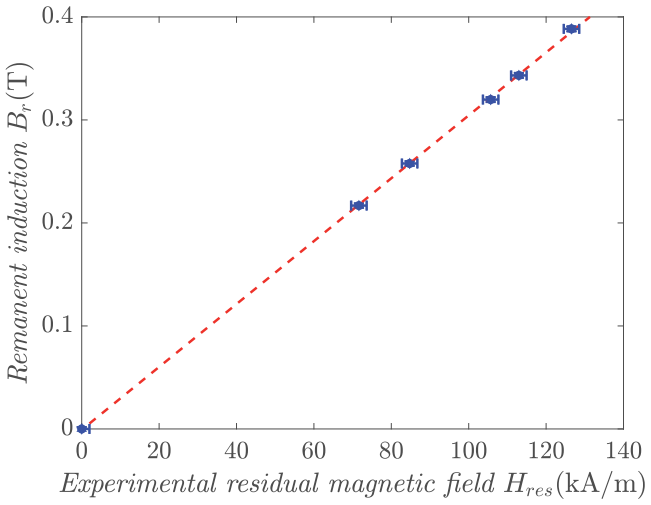

Fig. 4. Remanent induction B_r measured by the fluxmetric method as a function of the measured residual magnetic field H_{res} (dots) and corresponding linear interpolation (dashed line) for a 10 mm-diameter 10 mm-height cylindrical Ferrite magnet.

probe with the gaussmeter (BROCKHAUS Gaussmeter BGM 201) set to a measuring range of 400 mT for hard Ferrites and Sm–Co, and 4 T for Nd–Fe–B. The measuring accuracy provided by the manufacturer is ±0.5%, and the measured noise is ±2 kA/m and ±6 kA/m for the 400 mT and 4 T ranges, respectively.

A linear relation between the measured magnetic field on the surfaces H_{res} and the average remanent induction B_r in the specimen volume can be established. This relation depends on the sample dimensions and its recoil permeability μ_{rec}. The proportionality coefficient k linking H_{res} and B_r ($B_r = kH_{res}$) can be obtained for circular cylinders from an analytical integral expression [17] or through numerical simulation for more general cylindrical shapes. Here, the calculation was performed using the finite element software COMSOL (similar problem as defined in Appendix A). A uniformly magnetized cylinder was considered (uniform M_r), and the average value H_{res} of the residual magnetic field in a 1 mm^3 zone centered at the top and bottom surface of the sample was extracted. This zone simulates the active zone of a Hall probe. Fig. 3 shows the results for a 10 mm-diameter 10 mm-height cylinder with recoil permeability $\mu_{rec} = 1$.

The relationship between H_{res} and B_r is clearly linear, and the proportionality constant k, obtained from linear interpolation, is found, for these dimensions, to be equal to 3.14 10^{-6} kg m / A^2 s^2. Simulations for recoil permeabilities μ_{rec} ranging from 1 to 1.75 were conducted, corresponding to the values of most magnets. It was found that, for this range of recoil permeabilities, the proportionality factor k only depends on the sample geometry. The numerical method to determine k can be applied from the knowledge of the magnet geometry only.

The practical application of the method consists of applying three simple steps:

- measurement of the residual magnetic field H_{res} with a magnetic field sensor in the area of interest (top and bottom surfaces of the cylindrical magnet),
- identification of the proportionality parameter k using simulation,
- deduction of the magnetic induction using the relation $B_r = kH_{res}$.

2.5. Validation of the RMFM

Experimental tests were performed on a 10 mm-diameter and 10 mm-height Ferrite magnet in order to validate the method. The sample is initially demagnetized, as described in [15,16]. It is then magnetized at increasing induction levels, and the residual magnetic field and magnetic permeability μ are measured at each induction level. The residual field along the z-axis of the cylindrical sample is measured by placing the Hall probe in the central region of the top or bottom surface. The magnetic field there is reasonably uniform in a volume larger than the active zone of the Hall probe. This eliminates the need for an extreme accuracy in the positioning of the probe.

The experimental results are shown in Fig. 4.

The line is a linear interpolation. The observed proportionality coefficient k_{exp} is found equal to 3.08 10^{-6} kg m / A^2 s^2. The calculated proportionality coefficient k using the numerical simulation is k_{sim} =3.14 10^{-6} kg m / A^2 s^2, which is very close.

2.6. Application to the characterization of rare-earth magnets

The two proposed measurement techniques, MEM and RMFM, were applied to two types of rare-earth magnets, Neodymium–Iron–Boron (Nd–Fe–B) and Samarium-Cobalt (Sm–Co). For these high-performance magnets, the coercive fields are too high to allow an easy application of the fluxmetric method.

For the MEM, the extraction was repeated at least 5 times, so that the repeatability error is representative of all the error sources combined.

For the RMFM, the recoil magnetic permeabilities of the materials were obtained by applying a small sinusoidal field around the remanence state and calculated by the ratio $\frac{1}{\mu_0}\frac{\Delta B}{\Delta H}$. The obtained values are comprised between 1.1 and 1.6 for all types of magnets.

The results for the remanent induction are compared in Table 1 to the corresponding datasheet, and they fall within the range provided by the manufacturer. The data provided by the manufacturers is measured by standard methods and covers variability from different batches of samples. The measurement errors of the proposed approach appear to be included in the range provided by the manufacturer, connected to the variability in the production process. This comparison serves as a first validation attesting to the reliability of MEM and RMFM.

As an intermediate conclusion, two experimental techniques were proposed to estimate the remanent induction of permanent magnets. Both provided satisfying results. Errors not exceeding 4% for MEM and 2% for RMFM are reported, and are comparable to standard methods. The decisive advantage of MEM and RMFM resides in their low cost and ease of implementation. The MEM must be performed with great attention to the boundary conditions in the closed magnetic circuit,

Table 1
Remanent induction B_r obtained by MEM and RMFM on two rare-earth magnets and corresponding manufacturer data.

Magnet type	Measurement method	Measured remanent induction B_r (T)	Manufacturer data B_r (T)
Nd–Fe–B	MEM	1.38 ± 0.01	1.37–1.42
	RMFM	1.38 ± 0.02	
Sm-Co	MEM	0.99 ± 0.01	0.96–1.04
	RMFM	1.00 ± 0.01	

since an air gap in the circuit can lead to significant demagnetizing effects resulting in an underestimation of the remanent magnetization. Accurate estimation of flux variation measurement errors is also needed. On the other hand, the RMFM is very simple to implement and is subjected to less sources of systematic errors. Nevertheless, good knowledge of the field uniformity area must be obtained through finite element simulation, and errors and noise from the Hall probe must be monitored. The uniformity of the residual field in the measuring area is the only condition that makes the measurement by RMFM feasible.

The idea of the RMFM could be extended to be applied in real-time application. Contrarily to MEM, where a separation between the sample and its operational location is necessary for measurement. The MEM is applicable only if the sample can be put in a closed circuit with respect to the direction of its magnetization, and the flux variation measurement can be done during the extraction.

In the next section, MEM and RMFM are implemented to analyze the functional fatigue of permanent magnets subjected to cyclic mechanical loadings.

3. Experimental study of functional fatigue in permanent magnets

Several studies were devoted to the magneto-mechanical effects in magnetic materials. Experimental setups for the characterization of the effects of static stress on the magnetic behavior were developed [15,18–20]. Fewer studies investigated the effect of dynamic or cyclic mechanical stress on the magnetic behavior [21–23], focusing on soft magnetic materials only.

Even if purely mechanical behavior [24,25] and magneto-thermal couplings [26–28] have been studied in hard magnets, only few references address the magneto-mechanical coupling in hard magnetic materials. Takezawa et al. [29] examined the change in domain configuration induced by compressive stresses using a Kerr microscope and reported a demagnetization ratio of 0.14% in the observation field. Wang et al. [30] conducted an experimental research to test the characteristics of Nd–Fe–B and Sm–Co permanent magnets by emulating the stress and temperature conditions of high-speed machines: stress varying from 0 to −90 MPa (compressive stress) and temperatures from 25 °C to 110 °C. They reported little sensitivity of hard magnets to magneto-mechanical effects in the study conditions. Mito et al. [31] examined the high pressure effects (up to −4.3 GPa) on isotropic Nd–Fe–B magnets and detected alteration in the material properties as the coercive field increased and the saturation magnetization decreased due to the high pressure. These works demonstrates magneto-mechanical effects in hard magnets in the case of static mechanical loading, although for harsh conditions. One explanation of the relatively low effects observed in the cited works is the combination of high magneto-crystalline energy and low magnetostriction levels. Chen et al. [32] measured the magnetostriction of Nd–Fe–B and hard Ferrite magnets and reported maximum values of the longitudinal saturation magnetostriction of +52 10^{-6}, and −25 10^{-6}, respectively.

This work deals with the effect of cycling mechanical loading – at room temperature – on the magnetic properties of hard ferromagnetic materials.

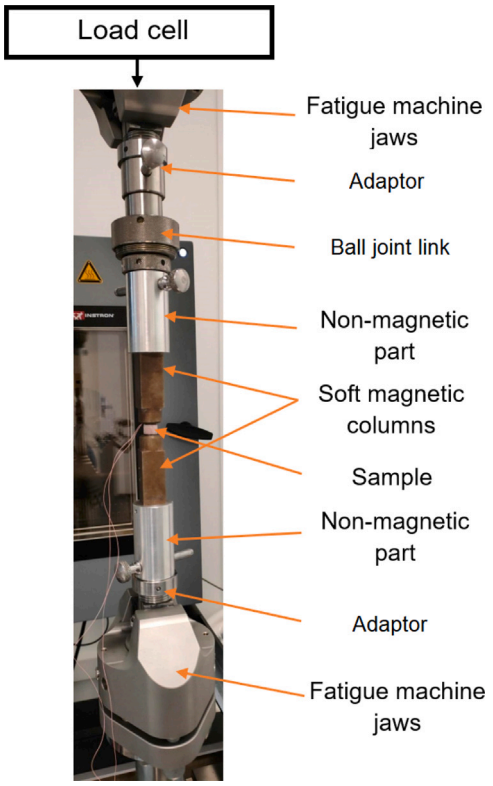

Fig. 5. Mechanical fatigue test setup.

3.1. Measurement device and protocol

The purpose of the experiment is to study the influence of applying cyclic compressive stress, below the compression yield stress of the studied material, on the remanent induction of magnet samples. The experimental procedure consists of first measuring the remanent induction of the sample. The subcritical cyclic compressive stress is then applied, after which, the remanent induction is measured again and compared to its initial value. The setup used for applying the stress is shown in Fig. 5.

The sample is placed between two soft magnetic and amagnetic columns forming an open circuit configuration. This configuration ensures a controlled environment for detecting magnetic variations while allowing mechanical stress to be applied. To apply the cyclic loading, the rig is inserted into a fatigue machine (Instron ElectroPuls E10000), ensuring precise force application with repeatable loading cycles.

The MEM and RMFM are used to assess the evolution of the remanent induction B_r of the samples, once unmounted from the fatigue rig. Three types of magnets were considered: hard Ferrites, Nd–Fe–B, and Sm–Co magnets. Three samples of each type were used. The samples were commercial 10 mm-diameter 10 mm-height cylinders for Ferrites and Nd–Fe–B, and commercial 9 mm-diameter 9 mm-height cylinders for Sm–Co. The mechanical loading path includes a (compressive) preload of −70 MPa (−85 MPa for Sm–Co) followed by a sequence of 10^6 sinusoidal cycles of amplitude 40 MPa (50 MPa for Sm–Co). The use of sinusoidal loading ensures a smooth and cyclic application of mechanical stress. The frequency was set to 30 Hz. The choice of the loading conditions was guided by [4–6,30] to match stress values and number of cycles in practical applications. The study is realized at room temperature with no temperature control and is limited to uniaxial compressive mechanical loadings.

3.2. Effect of cyclic stress on the remanent induction

The results of the experimental campaign are shown in Fig. 6, in which the evolution of remanent induction B_r measured by MEM and RMFM are plotted.

Differences can be first observed between MEM and RMFM measurements. RMFM results are systematically above MEM results. The major hypothesis of the MEM method is that the sample, when put in the closed circuit, is not subjected to any demagnetizing field. In practice, this hypothesis is verified only if there is no airgap in the closed circuit. An analysis of the experimental conditions showed the existence of small airgaps between the sample and the column. These airgaps lead to an underestimation of the measured flux variation and consequently the remanent induction was underestimated. For the same reason, it can also be noted that the repeatability of RMFM is usually better than that of MEM. These observations tend to promote the RMFM as a more accurate technique for the induction measurement.

Whatever the technique used, no significant change in remanent induction was observed after cycling. The recoil permeability measurements, not shown here, did not show any significant change either after cyclic loading.

The experimental approach followed in this study is similar to previous studies on soft magnetic materials, see for instance [6]. Compared to many soft magnetic materials, hard magnets show little sensitivity to stress. This low sensitivity to stress is attributed to their high magneto-crystalline anisotropy, preventing the magneto-elastic energy from significantly altering the energy balance.

4. Conclusion

Two novel techniques for estimating the remanent induction of hard ferromagnetic materials were presented. The modified extraction method (MEM) and the residual magnetic field method (RMFM) demonstrate good accuracy and reliability in measuring the remanent induction of magnets. RMFM exhibits less sources of systematic errors, and is thought to be more accurate. Although, the validation and application of the proposed methods were limited to cylindrical samples, it is possible to generalize them to a variety of regularly shaped samples with a broad range of dimensions. They can be applied to any hard magnetic material.

These techniques were applied to investigate the impact of cyclic mechanical loadings on the remanent induction of permanent magnets. In the considered range of mechanical loadings, representative for practical loadings in electrical machines, and at room temperature, none of the tested materials revealed significant functional fatigue. Such results support the robustness, long-term durability and reliability of the tested materials, making them appropriate for applications with dynamic mechanical loadings. Tests at higher temperatures, extreme mechanical loadings, or under mechanical impacts, however, may bring different conclusions. These points could be the object of future works, based on the proposed experimental protocol.

CRediT authorship contribution statement

Abderraouf Ouazib: Writing – review & editing, Writing – original draft, Conceptualization. **Mathieu Domenjoud:** Writing – review & editing, Conceptualization. **Laurent Daniel:** Writing – review & editing, Conceptualization.

Declaration of competing interest

The authors declare that they have no known competing financial interests or personal relationships that could have appeared to influence the work reported in this paper.

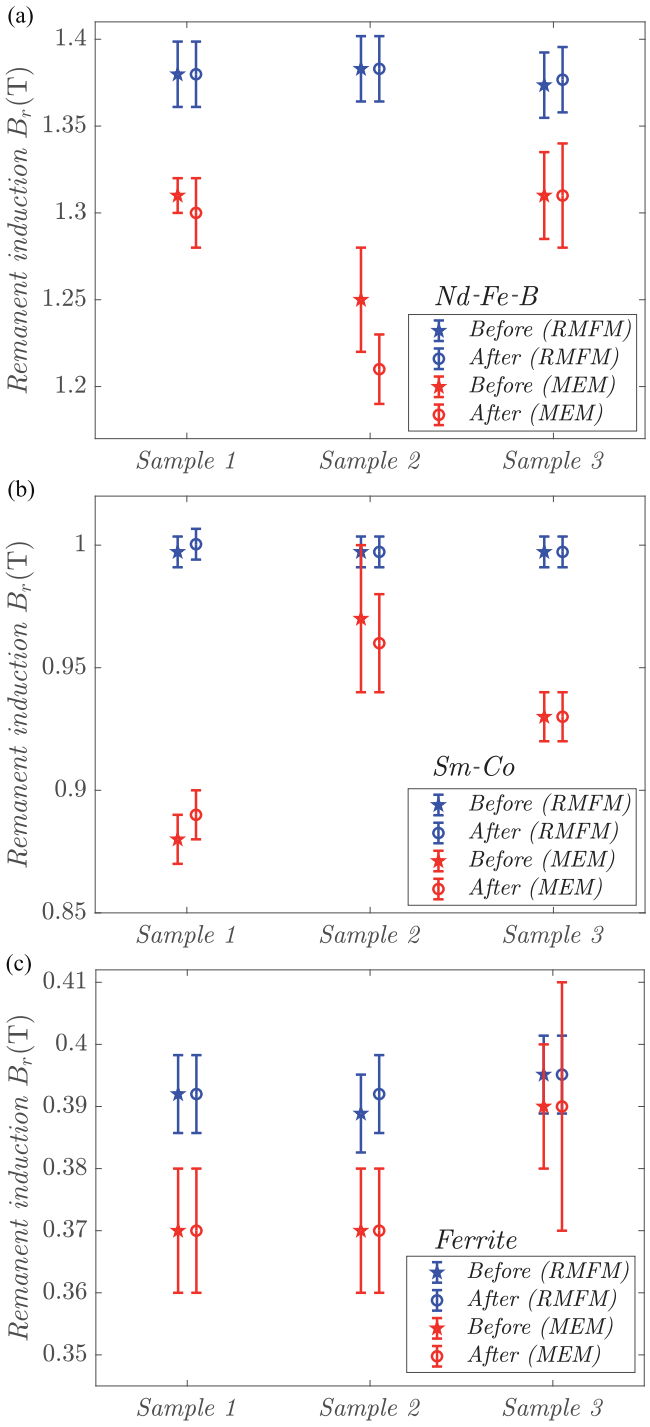

Fig. 6. Remanent induction B_r before and after cyclic mechanical loading (10^6 cycles) measured by modified extraction method (MEM) and by residual magnetic field method (RMFM) for Nd–Fe–B (a), Sm–Co (b) and hard Ferrite (c).

Appendix A. Estimation of the demagnetizing factors

Both MEM and RMFM require the calculation of demagnetizing factors. The demagnetizing factor is a proportionality coefficient between the uniform magnetization of an ellipsoid and the corresponding internal uniform demagnetizing field. Except for ellipsoids, there is no rigorous definition of the demagnetizing factor of uniformly magnetized bodies (because the demagnetizing field is not uniform within

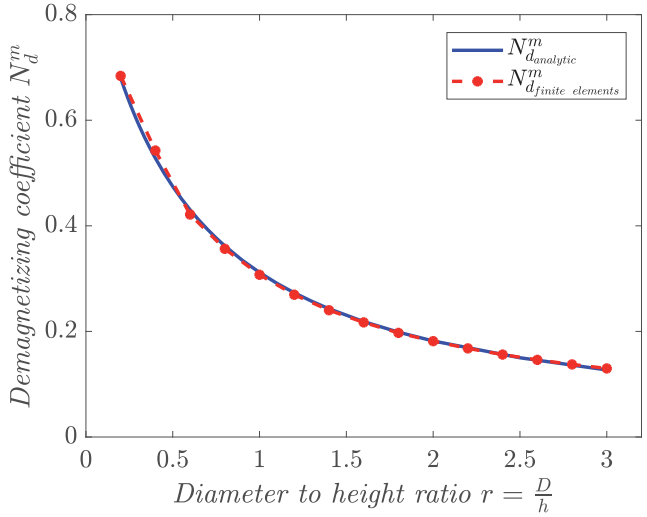

Fig. 7. Comparison between the evolution of the demagnetizing coefficient N_d^m calculated analytically [33] (in blue) and by finite element analysis (in red) as a function of diameter to height aspect ratio of the sample.

the sample). But the concept remains useful in some applications. Two possible definitions are considered in this article:

- the fluxmetric demagnetizing coefficient N_d^f is used in the classical extraction method (in the case of a short detection coil), defined as the average demagnetizing coefficient across the mid-section of the sample,
- the magnetometric demagnetizing coefficient N_d^m is used in the MEM and the RMFM, defined as the demagnetizing coefficient averaged over the volume of the sample.

The value of the demagnetizing factor depends on the dimensions and on the magnetic permeability of the studied sample. Under the assumption of a uniform magnetization M_r and knowing the value of recoil permeability μ_{rec}, strategies for calculating the demagnetizing field have been proposed in the literature. The fluxmetric (ballistic) and magnetometric demagnetizing factors of cylinders can be obtained as a function of the diameter-to-height ratio r using analytical 1D or 2D models [33,34]. They can also be estimated using finite element simulations [35] by calculating the distribution of the demagnetizing field H_d in a sample placed in vacuum and taking the ratio between the average of this field and the magnetization M_r of the magnet. In this study the FEM computation was conducted using COMSOL simulation software. As expected, this distribution is not strictly uniform, despite the uniformity of the magnetization, which explains the difficulty in accurately defining the demagnetizing coefficient. From such results the calculation of N_d^m was done by extracting the demagnetizing field values on a regular mesh from the obtained distribution. The ratio between the calculated average demagnetizing field H_d on this mesh and the magnetization M_r gives N_d^m. The simulation was performed for different dimensions (with different diameter-to-height ratio r), and the estimated coefficients were compared with the results of the analytical calculation in [33] for validation. The comparison results are shown in Fig. 7.

A very good agreement between the two calculation techniques is observed. When the ratio r is 1, which corresponds to the test configuration, the finite element analysis indicates $N_d = 0.307$, while the analytically calculated value in [33] is $N_d = 0.312$. The relative difference between these two results is less than 3%. Given this good agreement any of the two techniques can be employed. The N_d^m calculated by finite element method was chosen for the calculations of this article.

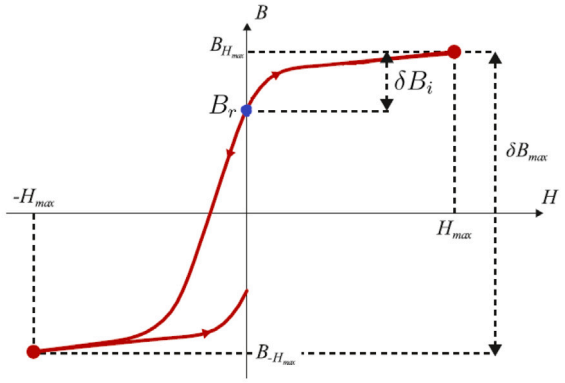

Fig. 8. Principle of the remanent induction B_r measurement from hysteresis loops.

Appendix B. Remanent induction measurement from hysteresis loops

The measurement of the remanent induction B_r from a hysteresis loop requires the measurement of the induction variations over a complete hysteresis loop starting from the remanent state of the material. In this study sinusoidal magnetic field was applied at a frequency of 1 Hz using the closed magnetic circuit described in Section 2.3.

Measured induction variation between $H = 0$ and H_{max} (the maximum applied field) starting from the remanent state gives the value of δB_i. δB_{max} is then obtained by measuring the induction variation between H_{max} and $-H_{max}$, as shown in Fig. 8.

The remanent induction value B_r is then calculated using the following relation:

$$B_r = -\frac{1}{2}\delta B_{max} - \delta B_i. \tag{4}$$

Data availability

No data was used for the research described in the article.

References

[1] S. Hirosawa, M. Nishino, S. Miyashita, Perspectives for high-performance permanent magnets: applications, coercivity, and new materials, Adv. Nat. Sci.: Nanosci. Nanotechnol. 8 (1) (2017) 013002.
[2] A.R. Tariq, C.E. Nino-Baron, E.G. Strangas, Consideration of magnet materials in the design of PMSMs for hevs application, in: 2011 IEEE Power and Energy Society General Meeting, IEEE, 2011, pp. 1–6.
[3] I. Petrov, J. Pyrhonen, Performance of low-cost permanent magnet material in PM synchronous machines, IEEE Trans. Ind. Electron. 60 (6) (2012) 2131–2138.
[4] A. Binder, T. Schneider, M. Klohr, Fixation of buried and surface-mounted magnets in high-speed permanent-magnet synchronous machines, IEEE Trans. Ind. Appl. 42 (4) (2006) 1031–1037.
[5] A. Borisavljevic, H. Polinder, J. Ferreira, Enclosure design for a high-speed permanent magnet rotor, 2010.
[6] J. Karthaus, K. Hameyer, Static and cyclic mechanical loads inside the rotor lamination of high-speed pmsm, in: 2017 7th International Electric Drives Production Conference, EDPC, IEEE, 2017, pp. 1–6.
[7] B.D. Cullity, C.D. Graham, Introduction to Magnetic Materials, John Wiley & Sons, 2011.
[8] Y. Liu, Discussion on several principal problems aroused from measuring high performance permanent magnetic materials, Int. J. Appl. Electromagn. Mech. 55 (3) (2017) 453–479.
[9] IEC-60404-5, Magnetic materials - part 5: Permanent magnet (magnetically hard) materials - methods of measurement of magnetic properties, 2015.
[10] F. Fiorillo, Measurement and Characterization of Magnetic Materials (Electromagnetism), Elsevier Academic Press, 2005.
[11] S. Trout, Use of Helmholtz coils for magnetic measurements, IEEE Trans. Magn. 24 (4) (1988) 2108–2111.
[12] S. Tumanski, Handbook of Magnetic Measurements, CRC Press, 2016.

[13] IEC-60404-14, Magnetic materials - part 14: Methods of measurement of the magnetic dipole moment of a ferromagnetic material specimen by the withdrawal or rotation method, 2002.
[14] D. Craik, The measurement of magnetization using hall probes, J. Phys. E: Sci. Instrum. 1 (12) (1968) 1193.
[15] M. Domenjoud, E. Berthelot, N. Galopin, R. Corcolle, Y. Bernard, L. Daniel, Characterization of giant magnetostrictive materials under static stress: influence of loading boundary conditions, Smart Mater. Struct. 28 (9) (2019) 095012.
[16] L. Daniel, M. Domenjoud, Anhysteretic magneto-elastic behaviour of Terfenol-D: Experiments, multiscale modelling and analytical formulas, Materials 14 (18) (2021) 5165.
[17] M. Jin, Magnetic induction strength on surface of a ferro-medium circular cylinder, Theor. Appl. Mech. Lett. 6 (5) (2016) 209–212.
[18] D. Jiles, Integrated on-line instrumentation for simultaneous automated measurement of magnetic field, induction, Barkhausen effect, magnetoacoustic emission, and magnetostriction, J. Appl. Phys. 63 (8) (1988) 3946–3948.
[19] L. Kvarnsjo, G. Engdahl, A set-up for dynamic measurements of magnetic and mechanical behavior of magnetostrictive materials, IEEE Trans. Magn. 25 (5) (1989) 4195–4197.
[20] M.B. Moffett, A.E. Clark, M. Wun-Fogle, J. Linberg, J.P. Teter, E.A. McLaughlin, Characterization of Terfenol-D for magnetostrictive transducers, J. Acoust. Soc. Am. 89 (3) (1991) 1448–1455.
[21] K. Prajapati, R. Greenough, A. Wharton, M. Stewart, M. Gee, Effect of cyclic stress on Terfenol-D, IEEE Trans. Magn. 32 (5) (1996) 4761–4763.
[22] O. Ghibaudo, H. Chazal, N. Galopin, L. Garbuio, Magnetic behavior measurements under high frequency mechanical solicitations, in: 2015 IEEE International Instrumentation and Measurement Technology Conference (I2MTC) Proceedings, IEEE, 2015, pp. 387–392.
[23] J. Karthaus, S. Steentjes, D. Gröbel, A. Kolja, M. Merklein, K. Hameyer, Influence of the mechanical fatigue progress on the magnetic properties of electrical steel sheets, Arch. Electr. Eng. 66 (2) (2017).
[24] L. Li, G. Yang, Q. Sun, Dynamic damage study of sintered NdFeB in electromagnetic buffer under intensive impact load: Experiments, numerical simulation, and interval uncertain optimization, Mech. Adv. Mater. Struct. 29 (24) (2022) 3523–3539.
[25] L. Li, G. Yang, L. Wang, Q. Wu, Experimental and theoretical model study on the dynamic mechanical behavior of sintered NdFeB, J. Alloys Compd. 890 (2022) 161787.
[26] P. Gaunt, Magnetic viscosity and thermal activation energy, J. Appl. Phys. 59 (12) (1986) 4129–4132.
[27] A.S. Nunes, L. Daniel, M. Hage-Hassan, M. Domenjoud, Modeling of the magnetic behavior of permanent magnets including ageing effects, J. Magn. Magn. Mater. 512 (2020) 166930.
[28] R. Street, R. Day, J. Dunlop, Magnetic viscosity in NdFeB and SmCo5 alloys, J. Magn. Magn. Mater. 69 (1) (1987) 106–112.
[29] M. Takezawa, Y. Morimoto, J. Ejima, Y. Nakano, T. Araki, Change in magnetic domain structure of Nd-Fe-B sintered magnets by compressive stress, Electr. Eng. Japan 203 (1) (2018) 9–17.
[30] Y. Wang, H. Cao, I. Colak, Y. Zhang, J. Shen, Experimental study on characteristics variation of permanent magnets for high-speed machine applications, Chin. J. Electr. Eng. 8 (1) (2022) 16–23.
[31] M. Mito, H. Goto, K. Nagai, K. Tsuruta, H. Deguchi, T. Tajiri, K. Konishi, High pressure effects on isotropic Nd2Fe14B magnet accompanying change in coercive field, J. Appl. Phys. 118 (14) (2015).
[32] H.-Y. Chen, Y. Zhang, Y.-B. Yang, X.-G. Chen, S.-Q. Liu, C.-S. Wang, Y.-C. Yang, J.-B. Yang, Magnetostrictions and magnetic properties of Nd-Fe-B and SrFe12O19, Chin. Phys. Lett. 28 (7) (2011) 077501.
[33] D.-X. Chen, J.A. Brug, R.B. Goldfarb, Demagnetizing factors for cylinders, IEEE Trans. Magn. 27 (4) (1991) 3601–3619.
[34] M. Beleggia, D. Vokoun, M. De Graef, Demagnetization factors for cylindrical shells and related shapes, J. Magn. Magn. Mater. 321 (9) (2009) 1306–1315.
[35] B. Pugh, D. Kramer, C. Chen, Demagnetizing factors for various geometries precisely determined using 3-D electromagnetic field simulation, IEEE Trans. Magn. 47 (10) (2011) 4100–4103.